Control of NTMs by ECCD on ASDEX Upgrade in view of ITER Application

H Zohm[1], G Gantenbein[2], F Leuterer[1], M Maraschek[1], E Poli[1], L Urso[1] and the ASDEX Upgrade Team

[1]Max-Planck-Institut für Plasmaphysik, D-85748 Garching, Germany, EURATOM Association
[2]Forschungszentrum Karlsruhe, IHM, D-76021 Karlsruhe, EURATOM Association

E-mail:zohm@ipp.mpg.de

Abstract. The predictions of the generalised Rutherford equation for the stabilisation of Neoclassical Tearing Modes (NTMs) are reviewed. They suggest that the stabilisation efficiency can be maximised by maximising the current density within the island, favouring narrow deposition over maximum total current. Also, for ITER, where it is expected that the minimum island size before stabilisation will be small with respect to the deposition width, a loss of efficiency for continuous injection is predicted, but can be recovered by phased injection with respect to the island's O-point. The paper compares in detail these predictions with dedicated experiments on ASDEX Upgrade and finds good qualitative agreement with the generalised Rutherford equation. For quantitative agreement, the experimental database is not yet firm enough. The conclusion for ITER is that j_{ECCD} should be optimised and that modulation capability of the gyrotrons should be foreseen to ensure optimum stabilisation efficiency in the small island regime.

1. Introduction

MHD instabilities limit the operational space of tokamaks [1]; their control is therefore of great interest for present day and future tokamaks, such as ITER. In conventional scenarios, the Neoclassical Tearing Mode (NTM) [2] may limit access to the β-values required for sufficient production of fusion power [3]. This resistive instability is due to the loss of pressure driven bootstrap current inside the island associated with it. It has been shown that the marginal island size W_{marg} above which the mode is metastable, i.e. may be excited by a finite seed island generated by other MHD perturbations, scales with normalised poloidal ion gyro radius ρ_{pi}* [4]. Thus, in ITER one expects metastable NTMs at very low β-values.

Based on recent experimental success in the area of control of NTMs [5], [6], [7], [8], ECCD is foreseen as an MHD control tool in ITER. The design of this system is based on our current physics understanding cast into the generalised Rutherford equation for stabilisation [9]. It is the aim of this paper to review the predictions arising from this equation and then assess their validity by comparing to experiments carried out in the ASDEX Upgrade tokamak.

2. Theoretical background

NTM stabilisation by ECCD is usually described by the generalised Rutherford equation for the temporal evolution of the island width W [2]:

$$\frac{\tau}{r_s}\frac{dW}{dt} = r_s\Delta' + c_{sat}6.34 r_s \frac{\mu_0 L_q}{B_p} f_{GGJ} j_{bs}\frac{1}{W} - c_{stab}32\frac{\mu_0 r_s L_q d}{B_p} j_{ECCD}\eta_{CD}\frac{1}{W^2} \tag{1}$$

The function η_{CD} depends on the ratio of W to the ECCD deposition 1/e width d (a Gaussian current profile of the ECCD component is assumed, $j_{ECCD} \sim exp(-(r-r_s)^2/d^2)$) and can be obtained by averaging the ECCD source function over the island flux surfaces [10]. The current density j_{ECCD} is the value that would be driven for continuous injection, i.e. any reduction of current due to power modulation is covered in η_{CD}. In Eqn. 1, we have neglected the small island physics that determines the island width W_{marg} below which dW/dt becomes negative even without any ECCD, mainly because the precise physics of this is not known. Candidates for this behaviour are incomplete pressure flattening [11], reduction of bootstrap drive in islands smaller than the ion banana width [12] or the polarisation current [13]. Also, the stabilising effect of j_{ECCD} on the equilibrium current profile via changing Δ' [14] is not incorporated. Thus, we will obtain upper limits for the power required for stabilisation. Finally, the term $f_{GGJ} = 1 - 1.37\left(q^2-1\right)/\, q^2 L_q r_s^{1/2} / R^{3/2}$ accounts for the reduction of the bootstrap drive by the Glasser-Greene-Johnson effect [15]. We note that in the small island limit, it will not have the same functional dependence on W as the bootstrap term [16] and may not be combined with it into a single term, but since we neglect small island terms here, we have adopted this form. For typical parameters of the (2,1) NTM, it has values of $f_{GGJ} \sim 0.7$-0.8.

Since all coefficients in Eqn. (1) have been derived in cylindrical geometry with large aspect ratio expansion, we have introduced two fitting parameters c_{sat} and c_{stab} to account for deviations due to geometry or possibly other physics not covered here. These coefficients should be determined from the experiment. Without ECCD, the saturated island width is given by

$$W_{sat} = c_{sat}6.34 f_{GGJ}\frac{\mu_0 L_q j_{bs}}{B_p\left(-\Delta'\right)} \tag{2}$$

allowing the determination of c_{sat} independent of c_{stab}. The latter can then be found from stabilisation experiments [17].

The requirement for complete stabilisation can then be derived by setting Eqn. (1) to zero:

$$-\frac{W}{W_{sat}} + 1 - 5.05\frac{c_{stab}}{f_{GGJ}c_{sat}}\frac{d}{W}\frac{j_{ECCD}}{j_{bs}}\eta_{CD} = 0 \tag{3}$$

In present day devices, we usually have $d \le W_{marg}$. In this case, all ECCD current is driven in the island and η_{CD} attains the limiting value of ~ 0.4 for both modulated or continuous application. This can be seen from Fig. 1 where we have plotted the efficiency for a very localised deposition as function of the helical angle at which it is injected. For narrow deposition (left panel in Fig. 1), this curve is not antisymmetric with respect to 90^o so that for a rotating mode, X-point modulation with 50% duty cycle (corresponding to integration from 0^o to 90^o) leads to very small value of η_{CD} whereas O-point modulation with 50% duty cycle (corresponding to integration from 90^o to 180^o) leads to only a slight reduction in the η_{CD} value, but delivers of course only 50% of driven current, thus leading to values slightly below 50% for both this case and the continuous case (which is the sum of the two integrals).

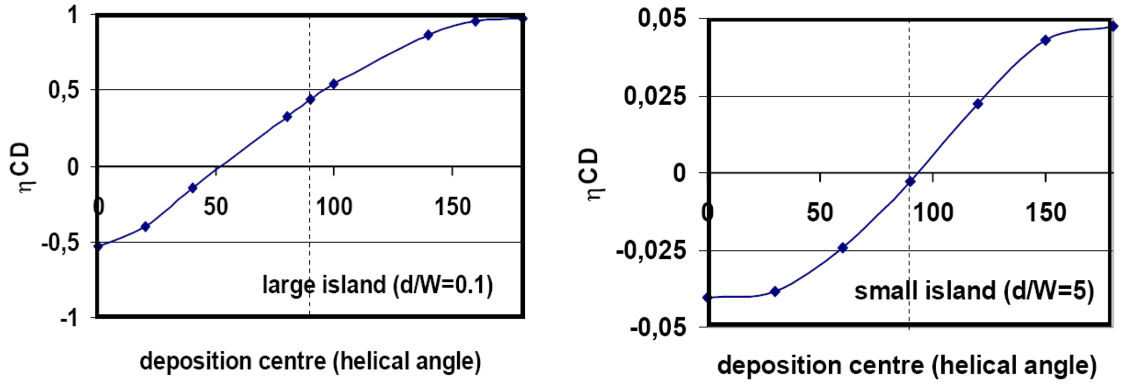

Figure 1. Stabilisation efficiency function η_{CD} for narrow (left) and broad (right) deposition for injection with highly localised helical angle range.

Thus, for continuous injection, postulating that no real root of Eqn. (3) exists (unconditional stability) leads to:

$$\frac{dj_{ECCD}}{W_{sat}j_{bs}} > \frac{1}{8} f_{GGJ} \frac{c_{sat}}{c_{stab}} \tag{4}$$

which is a condition on the total ECCD current relative to the total bootstrap current missing in the island. Since W_{sat} is proportional to j_{bs} (see Eqn. (2)), the current needed to stabilise NTMs scales quadratically with β in this case.

For ITER, the ρ*-scaling of W_{marg} leads to the expectation that $d > W_{marg}$. Then, for modulated CD within the island, only the current driven within the island counts, and we can approximate $\eta_{CD} \sim 0.15$ W/d. Furthermore, the first term of Eqn. (3) can be neglected at stabilisation (i.e. $W_{marg}/W_{sat} << 1$, which will be the case for relatively low β in ITER, while present day experiments do not necessarily operate in this regime), and unconditional stability is obtained for

$$\frac{j_{ECCD}}{j_{bs}} > 1.33 f_{GGJ} \frac{c_{sat}}{c_{stab}} \tag{5}$$

As pointed out before, f_{GGJ} is around 0.75 for typical cases so that this criterion just says that the local ECCD current density should exceed the bootstrap current density. This criterion has been adopted for the design of the ITER ECCD system for NTM stabilisation [9].

For continuous ECCD, the helical component is further reduced with respect to the modulated case, because current is also deposited around the X-point and the helical component is mainly generated in the island periphery around its separatrix. This reduction can be seen in the right panel of Fig. 1, where the curve is now more or less antisymmetric with respect to 90° so that integration from 90° to 180° (corresponding to phased O-point injection) will still give finite η_{CD} whereas integration from 0° to 180° (corresponding to continuous injection) gives a very small value. Then, the limit $\eta_{CD} \sim 1/8$ $(W/d)^2$ [10] applies and unconditional stability in Eqn. (4) can no longer be obtained. Assuming again that $W_{marg} << W_{sat}$, one obtains

$$\frac{j_{ECCD}}{j_{bs}} > 1.6 f_{GGJ} \frac{c_{sat}}{c_{stab}} \frac{d}{W} \tag{6}$$

i.e., for given j_{ECCD}, the NTM can only be reduced to a certain value of W. Inserting the value for complete stabilisation in the modulated case, one obtains $W = 1.2d$, i.e. the island can be reduced to a size comparable to the ECCD deposition width.

These predictions will are tested against experiments on ASDEX Upgrade in the next section.

3. Experiments on NTM Stabilisation

Experiments were carried out in ASDEX Upgrade lower single null H-mode discharges with ITER-like cross-section (R = 1.65 m, a = 0.5 m, $\kappa \approx 1.8$, $\delta \approx 0.2$, q_{95} = 3.5 - 4.5) in the density range of $n_e \approx$ 5 -6 x 10^{19} m^{-3}. NBI heating of 10-15 MW is applied to obtain β_N-values of 2.2-2.8, sufficient for the occurrence of (3,2) NTMs. The (2,1) NTM is not studied in this paper due to the higher power requirement for complete stabilisation that poses too strong restrictions on the operational range for the detailed studies presented here. The ASDEX Upgrade ECRH system is applied at 140 GHz in 2nd harmonic X-mode, i.e. resonant at 2.5 T. For the typical central field of B_t = 2.0 - 2.1 T used in these discharges, this results in high field side deposition. Slow ramps of B_t (about 10% within 2 seconds) are applied to sweep the deposition over the q = 1.5 surface, ensuring correct deposition within the sweep.

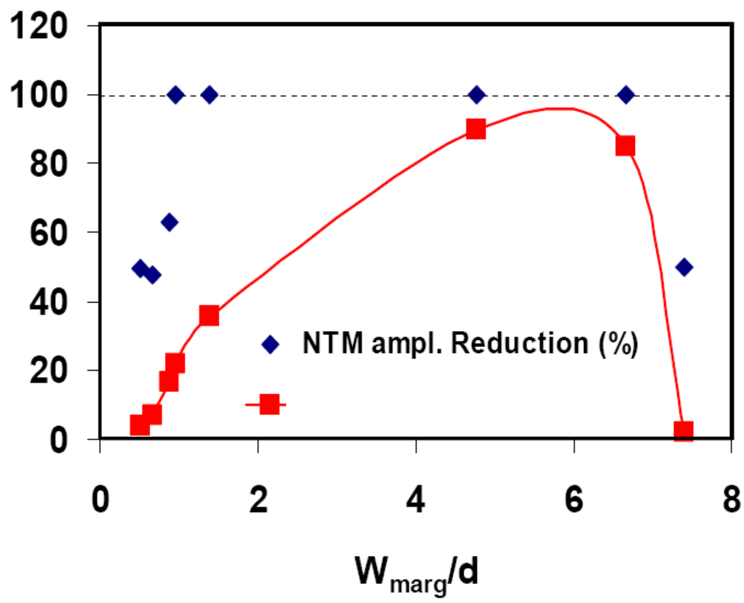

Figure 2. Scan of the deposition width during (3,2) NTM stabilisation by variation of the toroidal injection angle. For small deposition width (W_{marg}/d > 1), complete stabilisation (100% reduction) occurs while broad deposition results in partial stabilisation only. The drop of $j_{ECCD}\ \eta_{CD}$ at very narrow deposition is due to the perpendicular injection used in this discharge ($j_{ECCD} \Rightarrow 0$).

Previous experiments had proven that for the usually used deposition width ($W_{marg} \sim d$), it was not necessary to modulate the ECCD power to achieve complete stabilisation [6]. In fact, early experiments comparing phased and continuous injection at $d < W_{marg}$ showed no significant difference between the two, consistent with the prediction by the Rutherford equation outlined above. In order to assess the effect of the deposition width, a scan in toroidal injection angle under otherwards identical conditions was performed [18], leading to a simultaneous variation of the driven current and the deposition width. The results are shown in Fig. 2, where $j_{ECCD} \cdot \eta_{CD}$, the effective helical current density entering into the stabilisation term in the generalised Rutherford equation is compared with the reduction in mode amplitude observed in the experiment as function of the normalised deposition width (note that here, W_{marg} has been fixed to 2 cm). As predicted by the generalised Rutherford equation, complete stabilisation (100% reduction) occurs for large enough W_{marg}/d, whereas for small W_{marg}/d, only partial stabilisation is achieved, although these are the cases with largest toroidal injection angle, i.e. highest I_{ECCD}. This clearly proves the significance of the figure of merit $j_{ECCD} \cdot \eta_{CD}$ rather than the total current.

According to the consideration from section 2, the loss of stabilisation efficiency can be recovered by phased injection. Thus, a series of experiments was recently carried out using phased injection (for technical details, see [18]).

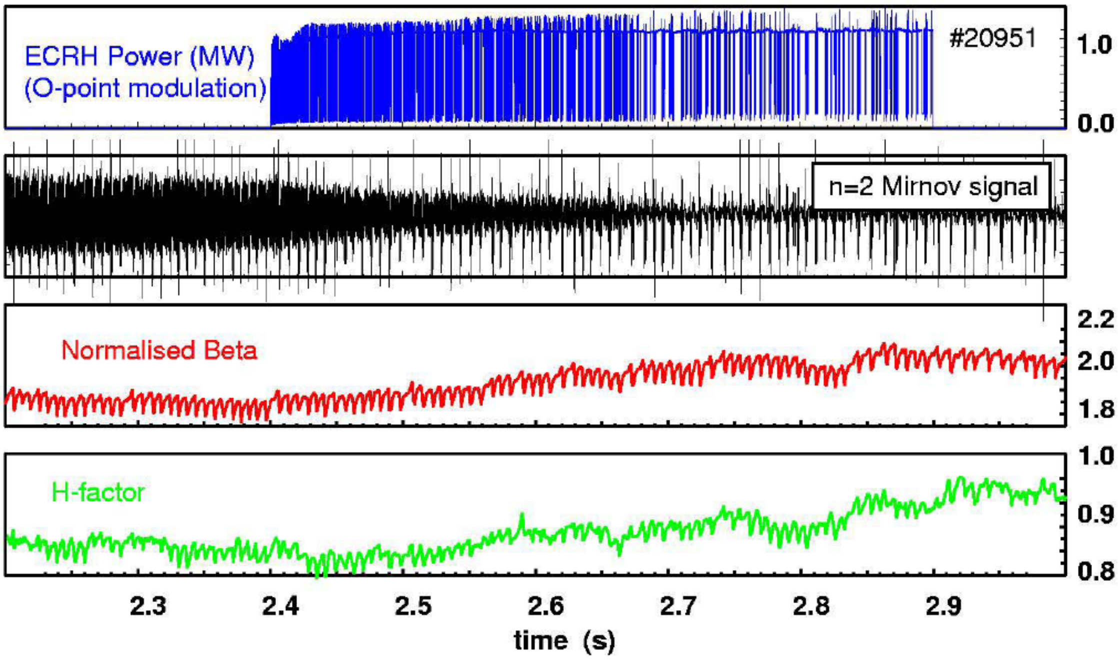

Figure 3. NTM stabilisation with broad deposition (W_{marg}/d = 0.75) and phased O-point injection, corresponding to the data point with 50% mode amplitude reduction in Fig. 2 (i.e. for continuous injection). Here, complete stabilisation occurs. During the whole phase shown here, ELMs introduce a modulation of the plasma parameters with a frequency of approximately 150 Hz.

For the phase in Fig. 3, which is estimated to be about 15^{o} shifted with respect to the O-point, full stabilisation is observed under conditions where with continuous injection, the reduction in mode amplitude was only about 50%. This phasing was then varied and the reduction in mode amplitude is shown in Fig. 4. Only the O-point phasing leads to complete stabilisation. The calculated efficiency function η_{CD} is also shown. This quantity has a maximum at O-point injection and a minimum for X-point injection (180^{o}). Reasonable agreement between the theoretical curve and the experimental data is achieved.

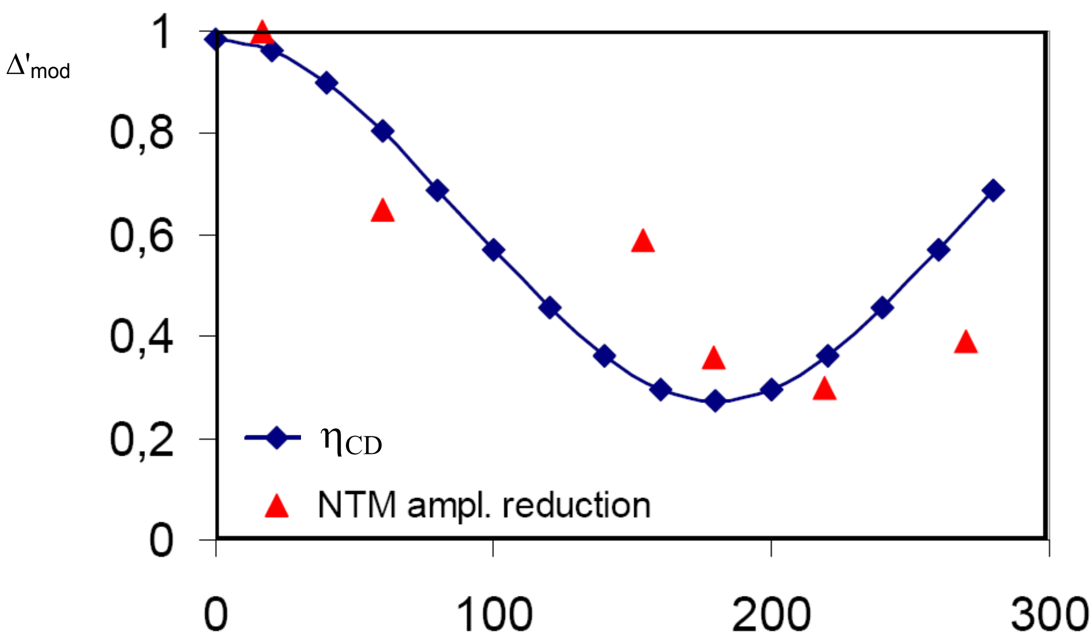

Figure 4. Experimentally observed mode amplitude reduction as function of the phase angle between ECCD and magnetic island. The efficiency function η_{CD} is also plotted, scaled and with an offset correction to account for the fact that stabilisation is also observed for X-point injection, where η_{CD} from flux surface averaging would be negative.

However, contrary to the expectation from section 2, the mode is still stabilised with X-point injection instead of being destabilised. The physical interpretation of this offset is that ECCD will also modify the equilibrium current profile, altering stability via the change in Δ' as discussed in [19]. As explained there, the modified stabilising term is of the form

$$\Delta'_{mod} \sim I_{ECCD}(\eta_{CD}\,(d/W)^2 + c_{00}) \tag{7}$$

where c_{00} is related to the (0,0) component of the current created by ECCD, affecting Δ'. This function is also shown in Fig. 4, with c_{00} = 0.13 to obtain a match between the NTM amplitude reduction and Δ'_{mod}.

From these comparisons, it is clear that the qualitative agreement between the dependency of η_{CD} and the experimental observations is very good for both $d > W_{marg}$ and $d < W_{marg}$, including the effects of phase injection. It remains to be seen if also quantitative agreement between the Rutherford equation for stabilisation and the experimental data can be obtained. To this end, we have determined the coefficient c_{sat} for a number of ASDEX Upgrade discharges from the saturated island width via relation (2). The results are plotted in Fig. 5.

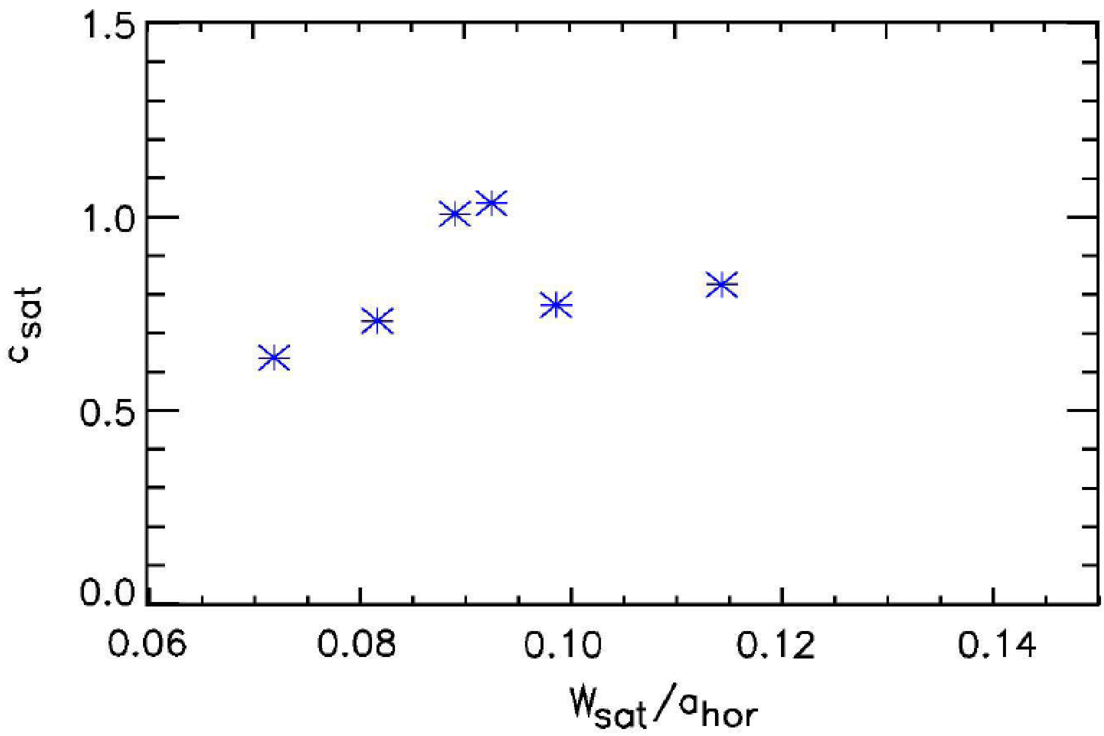

Figure 5. Fitting parameter c_{sat} for several ASDEX Upgrade discharges with a significant variation of the island width. c_{sat} is approximately constant with a value of approximately 0.8.

It can be seen that c_{sat} shows reasonably low scatter for a variation of the island width of almost a factor of two, with numerical value around 0.8. Unfortunately, the determination of c_{stab} is not as straightforward, because at stabilisation, it is not clear that the applied power was just marginal or exceeded that needed for marginality. In fact, also Fig. 2 suggests that in ASDEX Upgrade, the applied power is often significantly above marginal (up to a factor of two). In [11], therefore a value of $c_{stab} = 0.31$ has been deduced assuming marginality, while $c_{stab} = 1$ was inferred in [20] under the assumption that considerable mismatch in deposition exists in present day experiments. Inserting these values for c_{sat} and c_{stab} in to Eqn. (5) leads to a large uncertainty $0.8 < j_{ECCD}/j_{bs} < 2.5$ that is clearly not acceptable for extrapolation to ITER. More work is needed here, including fine scans of ECCD power to find the marginal point as well as multi-machine comparisons such as in [20] to narrow down the prediction.

4. Conclusions and Outlook

Dedicated experiments on ASDEX Upgrade show good qualitative agreement between the generalised Rutherford equation on NTM stabilisation and the experimental results. In particular, the role of the efficiency function η_{CD} that describes how efficient helical current is generated for a Gaussian ECCD deposition by flux surface averaging in the island is found to give a good description in the full parameter range studied, including present day experiments with $W_{marg} < d$ as well as the expected ITER range with $W_{marg} > d$. This includes the effect of modulation, which offers significant advantage in the ITER regime. While the validity of the figure of merit j_{ECCD}/j_{bs} for ITER is confirmed by our analysis, a prediction of power requirement still has large error bars, mainly due to the uncertainty about the marginal power level in present day experiments, which may overstabilise by large margins or, equivalently, operate with significant mismatch in deposition. Future experiments planned on ASDEX Upgrade and other devices will resolve this question.

Connected to the question of exact deposition is the need to feedback control the deposition. Also in this area, experiments are under way, including the extension of the ASDEX Upgrade ECRH system to 4 MW, 10 s, with variable frequency and fast (50 ms) steerable launchers.

5. References

[1] Zohm H et al. 2005 *Plasma Phys. Control. Fusion* **45** A163.

[2] Sauter O et al. 1997 *Phys. of Plasmas* **4** 1654.

[3] Sauter O and Zohm H *Proc. of the 26th EPS conference on Plasma Physics* 2005 Tarragona, Spain, ECA, Vol. **29C** P-2.059.

[4] Günter S et al. 1998 *Nucl. Fusion* **38** 1431.

[5] Zohm H et al. 1999 *Nucl. Fusion* **39** 577.

[6] Gantenbein G et al. 2000 *Phys. Rev. Lett.* **85** 1242.

[7] Isayama A et al. 2000 *Plasma Phys. Control. Fusion* **42** L37.

[8] La Haye R J et al. 2002 *Phys. Plasmas* **9** 2051.

[9] Zohm H et al. 2005 *J. Phys.: Conf. Ser.* **25** 234.

[10] Hegna C C et al. 1997 *Phys. Plasmas* **4** 2940.

[11] Fitzpatrick R 1995 *Phys. Plasmas* **2** 825.

[12] Poli E et al. 2002 *Phys. Rev. Lett.* **88** 075001-1.

[13] Wilson H et al. 1996 *Phys. Plasmas* **3** 248.

[14] Pletzer A and Perkins F 1999 *Phys. Plasmas* **6** 1589.

[15] Glasser A H et al. 1975 *Phys. Fluids* **12** 875.

[16] Lütjens H et al. 2001 *Phys. Plasmas* **8** 4267.

[17] Urso L et al. 2005 *J. Phys.: Conf. Ser.* **25** 266.

[18] Maraschek M et al. 2007 *Phys. Rev. Lett.* **98** 02005.

[19] Zohm H et al. 2007 *Nucl. Fusion* **47** 228.

[20] La Haye R J et al. 2006 *Nucl. Fusion* **46** 451.